Fluorescence Nanothermometers | Hot Paper

DOI: 10.1002/anie.201306366

Intracellular Thermometry by Using Fluorescent Gold Nanoclusters**

*Li Shang, Florian Stockmar, Naghmeh Azadfar, and G. Ulrich Nienhaus**

Cellular processes are exquisitely temperature-dependent because temperature governs the dynamics and reactivity of the vast number of biomolecules inside cells.[1] Therefore, accurate measurement of the cell temperature and its variation within the cell may contribute to advancements in cell biology and biomedicine.[2] To this end, fluorescence-based nanothermometers are of particular interest because they operate as "non-contact" devices and provide the dual function of imaging and temperature sensing at the nanoscale.[3] Indeed, several fluorescent nanomaterials, such as semiconductor quantum dots (QDs),[4] rare earth-doped nanoparticles,[5] and polymer-based nanogels[6] have already shown great potential for nanothermometry in biological systems, and especially live cells. For example, Lin et al.[7] have reported the capability of QDs of revealing spatially heterogeneous heat production in living cells.

Fluorescent gold nanoclusters (AuNCs) have recently gained considerable attention. Owing to their ultrasmall size (<2 nm in diameter), colloidal stability, good biocompatibility, and facile synthesis,[8] AuNCs are attractive for a wide variety of biomedical applications, such as biosensing,[9] in vitro and in vivo imaging,[10] and also in cancer therapy.[11] Herein, we present the use of AuNCs as versatile nanothermometry devices by taking advantage of the temperature sensitivity of their fluorescence lifetime and emission intensity, which change considerably over the physiological temperature range (15–45 °C). By using time-correlated single-photon counting (TCSPC)-based fluorescence lifetime imaging microscopy (FLIM), we demonstrate the great potential of AuNCs for spatially resolved temperature measurements in living cells.

[*] Dr. L. Shang, F. Stockmar, N. Azadfar, Prof. Dr. G. U. Nienhaus
Institute of Applied Physics and Center for Functional Nanostructures (CFN), Karlsruhe Institute of Technology (KIT)
76131 Karlsruhe (Germany)
E-mail: uli.nienhaus@kit.edu
Homepage: http://www.aph.kit.edu/nienhaus/
Prof. Dr. G. U. Nienhaus
Institute of Toxicology and Genetics
Karlsruhe Institute of Technology (KIT)
76344 Eggenstein-Leopoldshafen (Germany)
Prof. Dr. G. U. Nienhaus
Department of Physics, University of Illinois at Urbana-Champaign
Urbana, IL 61801 (USA)

[**] Financial support from the Deutsche Forschungsgemeinschaft (DFG) through the Center for Functional Nanostructures (CFN) and the Priority Program SPP1313 is gratefully acknowledged. We also thank Radian Popescu and Prof. Dr. Dagmar Gerthsen for their support with the HRTEM measurements, and Alexander Hepting for his help with building the temperature-controlled microscope sample stage.

Supporting information for this article is available on the WWW under http://dx.doi.org/10.1002/anie.201306366.

We synthesized lipoic acid-protected AuNCs according to a previously reported method.[12] These AuNCs possess a diameter of (1.6 ± 0.3) nm (Supporting Information, Figures S1 and S2) and emit bright fluorescence in the near-IR region. Importantly, they exhibit excellent colloidal stability in biological media, which is crucial for the performance of fluorescence probes in their biological applications.[13]

Figure 1 A shows the pronounced temperature dependence of the steady-state fluorescence emission spectra of the AuNCs in phosphate-buffered saline (PBS). The intensity decreases by 67 % upon raising the temperature from 10 to

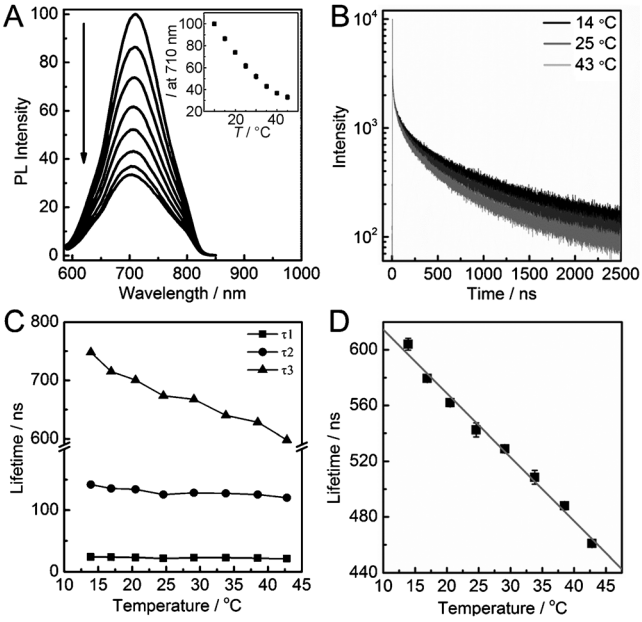

Figure 1. Temperature dependence of the fluorescence emission from lipoic acid-capped AuNCs dissolved in PBS. A) Fluorescence emission spectra (excitation 580 nm) for various temperatures in the range 10–45 °C (top to bottom). In the inset, the intensity at 710 nm is plotted versus temperature. B) Fluorescence emission decays at 14 °C (black curve), 25 °C (gray curve), 43 °C (light gray curve). C) Temperature dependence of the lifetimes of the three exponentials required to fit the fluorescence decay curves. D) Average fluorescence lifetime versus temperature and the corresponding linear regression (gray line).

45 °C. The temperature resolution is about 0.1–0.3 °C in this temperature range, assuming that an intensity change of 0.5 % $°C^{-1}$ is required to resolve a temperature difference.[14] Unlike QDs, which display remarkable temperature-dependent spectral shifts,[4a,7] the emission spectra of AuNCs do not shift within the investigated temperature window.

Concomitant with the intensity decrease, the fluorescence decay of AuNCs accelerates with increasing temperature (Figure 1 B). Lipoic acid-protected AuNCs display a charac-

teristic, nonexponential fluorescence decay that can be fitted with a sum of three exponentials, with a short ($\tau_1 \approx 24$ ns), a medium ($\tau_2 \approx 130$ ns), and a long lifetime (600 ns $< \tau_3 <$ 750 ns). The main contribution to the thermal response of AuNCs originates from the slow lifetime component, which dominates the overall temperature dependence (Figure 1C). The luminescence mechanism of these AuNCs is not yet fully understood. Previous studies on thiolated AuNCs indicated that the slow lifetime component, with τ_3 typically > 500 ns, is associated with the gold(I)–thiolate complex on the AuNC surface.[15] The average lifetime of AuNCs changes close to linearly with temperature; the fit yields a correlation coefficient of 0.9952 (Figure 1D). Therefore, not only the emission intensity, but also the average lifetime changes sensitively with temperature. The fluorescence lifetime is even more attractive for biological thermometry applications because, unlike intensity-based measurements, it is invariant to the local probe concentration or changes in fluorescence excitation conditions. Moreover, the average lifetime of AuNCs at room temperature is more than 500 ns; that is, two orders of magnitude above the lifetime of cellular autofluorescence. Therefore, AuNCs in biological samples can be imaged without any autofluorescence background by using FLIM with lifetime gating.[16] We note, however, that the long fluorescence lifetime slows data acquisition.

We have explored the capability of AuNCs for temperature sensing in HeLa human cancer cells using FLIM. Lipoic acid-capped AuNCs can be efficiently internalized by HeLa cells by energy-dependent, clathrin-mediated endocytosis.[17] Upon incubation with AuNCs (20 μg mL^{-1}) in serum-free cell culture medium for 2 h, appreciable amounts of AuNCs were observed inside the HeLa cells, as was also confirmed by intensity-based confocal microscopy (Supporting Information, Figure S3). We then varied the temperature of the environment of the HeLa cells by using a temperature-controlled sample stage. Lifetime maps were calculated on a pixel-by-pixel basis by fitting the fluorescence decay of each pixel with a tri-exponential function (Figure 2). These images provide clear evidence that the long fluorescence lifetime components in the range of 600–1000 ns arise from internalized AuNCs rather than cellular autofluorescence. With increasing temperature, the fluorescence lifetime decreased markedly. In fact, the intensity-weighted average lifetime of AuNCs dropped from 970 ns at 14 °C to 670 ns at 43 °C.

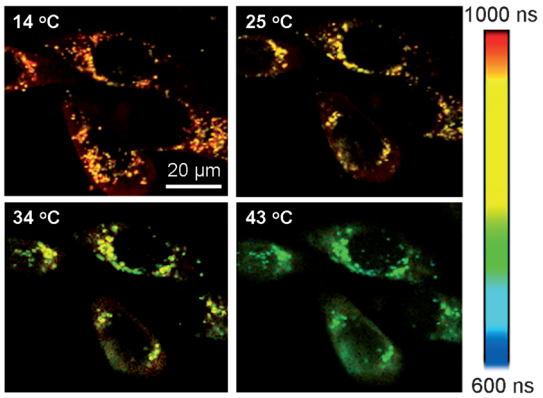

Figure 2. Typical FLIM images of HeLa cells with internalized AuNCs at four different temperatures.

Figure 3 shows that the fluorescence lifetime of AuNCs in HeLa cells is not sharply defined but distributed. Besides the intrinsic heterogeneity of the bare AuNCs, additional contributions arise from heterogeneous local chemical environments within the cells (Supporting Information, Figure S4 and Table S1).[2b,7,18]

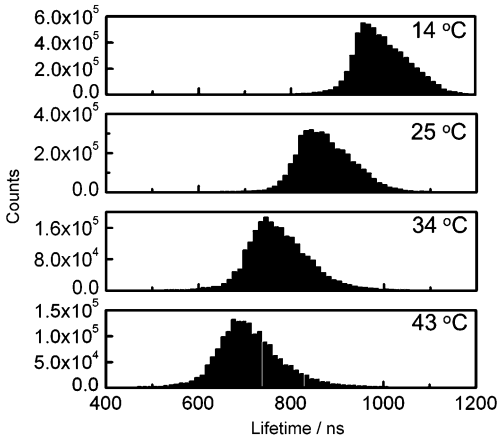

Figure 3. Average lifetime histograms of intracellular AuNCs at different temperatures, as obtained from FLIM images of HeLa cells.

Remarkably, the fluorescence lifetime of AuNCs is much larger in cells than in buffer solution over the entire temperature range studied. This effect most likely arises from the formation of a biomolecular corona around the internalized nanoparticles that modifies their photophysical properties.[19] Indeed, the in vitro analysis of the temperature response of AuNCs in the presence of serum proteins showed a prolonged fluorescence lifetime (Supporting Information, Figure S5). Recent studies revealed that protein adsorption can lead to significant changes of the photophysical properties of fluorescent nanoparticles.[20] The drastic changes of the fluorescence lifetime (including its temperature dependence) between cellular and buffer environment reported here for AuNCs underscore that the effects of nano–bio interactions have to be considered when designing fluorescent nanomaterials for bio-applications, for example, thermometry in cells.[4c,21]

We have carefully assessed the performance of our AuNCs for intracellular nanothermometry. Although we have not yet reached single-particle sensitivity, we can sensitively probe local cell temperature variations by analyzing the average lifetime of small ensembles. Indeed, the temperature resolution, based on the thermal response of AuNCs in HeLa cells (Figure 4A), is about 0.3–0.5 °C in the range 14–43 °C. Thus, our AuNCs compare well with other nanoparticle-based fluorescent thermometers[4b,5a,6] and are even superior to many molecule-based optical thermometers (Supporting Information, Table S2).[22] Importantly, under continuous excitation with intensities up to 2.8 kW cm^{-2} for 2 h, the fluorescence lifetime of AuNCs inside HeLa cells remained essentially constant (< 5% change, Figure 4B).

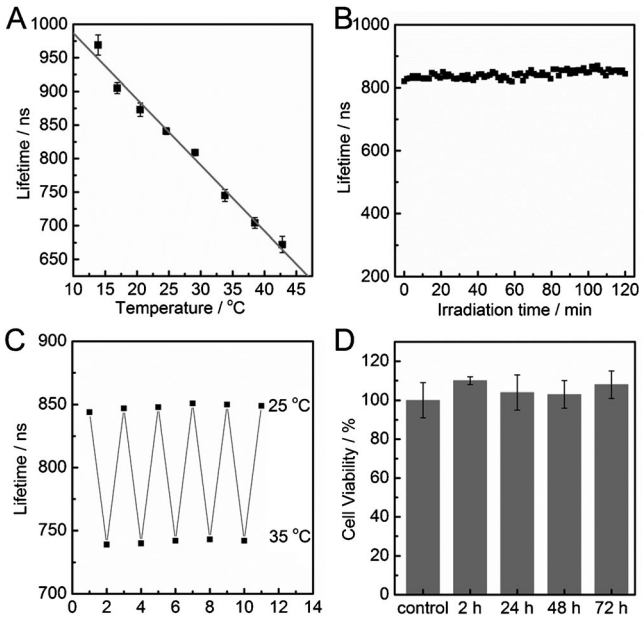

Figure 4. Performance assessment of AuNC-based fluorescence thermometry on HeLa cells. A) Average fluorescence lifetime of intracellular AuNCs versus temperature and the corresponding linear fit (line). B) Fluorescence lifetime of intracellular AuNCs as a function of irradiation time. The excitation intensity was kept constant at 2.8 kW cm^{-2}. C) Lifetime of intracellular AuNCs upon cycling the temperature five times between 25 and 35 °C. D) Viability of HeLa cells in cell medium as a function of time, as determined by an MTT assay. The cells were loaded with AuNCs prior to starting the experiment. The error bars represent variations among three independent measurements.

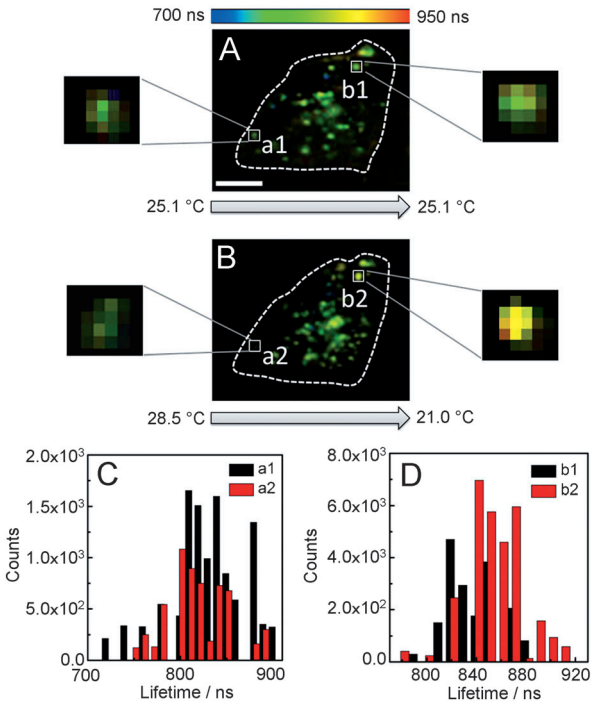

Figure 5. AuNC-based fluorescence thermometry of temperature variations inside HeLa cells. Typical fluorescence lifetime images of a HeLa cell with incorporated AuNCs are shown taken A) at constant temperature and B) in the presence of a temperature gradient across the cell; scale bar 10 μm. The temperatures quoted below the images are based on the calibration curve in Figure 4A. C), D) Lifetime distributions of two selected clusters of AuNCs inside the cells at constant temperature (a1 and b1) and in the presence of a temperature gradient (a2 and b2).

Moreover, the thermal response of AuNCs is completely reversible upon temperature cycling, and there is no thermal hysteresis during heating and cooling cycles, as shown for five cycles between 25 and 35 °C in Figure 4C. Finally, a thiazoyl blue tetrazolium bromide (MTT) assay showed no adverse effects to HeLa cells within 72 h after AuNC exposure (Figure 4D), suggesting an excellent biocompatibility of our intracellular nanothermometers. Taken together, our AuNC-based system is among the most versatile optical thermometers reported to date.[3b,5c,7]

We also explored the capability of our AuNC-based nanothermometers to detect intracellular temperature differences in HeLa cells. By using a specially designed sample stage (Supporting Information, Scheme S1 and Figure S6), we applied a temperature gradient across the cells. As expected, the spatial lifetime profile of the cell was observed to change depending on the horizontal position (Figure 5). For a detailed analysis, we selected two clusters of AuNCs, denoted by (a) and (b) in the figure, with average lifetimes of about 834 ns at 25.1 °C. After establishing a temperature gradient, the lifetime of cluster (a) decreased to 815 ns, corresponding to a temperature increase by 1.9 °C, calculated by using the calibration curve in Figure 4A. The lifetime of cluster (b), however, increased to 854 ns, indicating a temperature decrease by 2.0 °C. The results thus confirm the potential of our AuNC-based system for sensing temperature profiles at the subcellular level.

In conclusion, we have reported on the application of fluorescent AuNCs to intracellular temperature sensing. These nanothermometers feature a high temperature sensitivity of both their fluorescence intensity and lifetime and an excellent stability over the physiological temperature range. They enable precise temperature measurements in biological systems in a spatially resolved fashion by using fluorescence imaging. In the current study, AuNCs were incorporated into the cells by simple endocytosis and ended up mainly in endosomes/lysosomes. Further work aimed at delivering these nanothermometers to other cell organelles is ongoing. Also, the combination of these fluorescent nanothermometers with super-resolution optical microscopy[23] can be envisioned.

Received: July 22, 2013
Published online: September 13, 2013

Keywords: fluorescence · gold nanoclusters · imaging · sensors · temperature

[1] a) M. Monti, L. Brandt, J. Ikomi-Kumm, H. Olsson, *Scand. J. Haematol.* **1986**, *36*, 353–357; b) O. Zohar, M. Ikeda, H. Shinagawa, H. Inoue, H. Nakamura, D. Elbaum, D. L. Alkon, T. Yoshioka, *Biophys. J.* **1998**, *74*, 82–89; c) B. B. Lowell, B. M.

Spiegelman, *Nature* **2000**, *404*, 652 – 660; d) M. Guo, Y. Xu, M. Gruebele, *Proc. Natl. Acad. Sci. USA* **2012**, *109*, 17863 – 17867.
[2] a) K. M. McCabe, M. Hernandez, *Pediatr. Res.* **2010**, *67*, 469 – 475; b) K. Okabe, N. Inada, C. Gota, Y. Harada, T. Funatsu, S. Uchiyama, *Nat. Commun.* **2012**, *3*, 705.
[3] a) J. Lee, N. A. Kotov, *Nano Today* **2007**, *2*, 48 – 51; b) D. Jaque, F. Vetrone, *Nanoscale* **2012**, *4*, 4301 – 4326.
[4] a) L. Martinez Maestro, E. Martín Rodríguez, F. Sanz-Rodríguez, M. C. Iglesias de La Cruz, A. Juarranz, R. Naccache, F. Vetrone, D. Jaque, J. A. Capobianco, J. García Solé, *Nano Lett.* **2010**, *10*, 5109 – 5115; b) L. M. Maestro, C. Jacinto, U. R. Silva, F. Vetrone, J. A. Capobianco, D. Jaque, J. G. Solé, *Small* **2011**, *7*, 1774 – 1778; c) A. E. Albers, E. M. Chan, P. M. McBride, C. M. Ajo-Franklin, B. E. Cohen, B. A. Helms, *J. Am. Chem. Soc.* **2012**, *134*, 9565 – 9568.
[5] a) H. S. Peng, M. I. J. Stich, J. B. Yu, L. N. Sun, L. H. Fischer, O. S. Wolfbeis, *Adv. Mater.* **2010**, *22*, 716 – 719; b) F. Vetrone, R. Naccache, A. Zamarrón, A. Juarranz de La Fuente, F. Sanz-Rodríguez, L. Martínez Maestro, E. Martín Rodriguez, D. Jaque, J. García Solé, J. A. Capobianco, *ACS Nano* **2010**, *4*, 3254 – 3258; c) L. H. Fischer, G. S. Harms, O. S. Wolfbeis, *Angew. Chem.* **2011**, *123*, 4640 – 4645; *Angew. Chem. Int. Ed.* **2011**, *50*, 4546 – 4551.
[6] C. Gota, K. Okabe, T. Funatsu, Y. Harada, S. Uchiyama, *J. Am. Chem. Soc.* **2009**, *131*, 2766 – 2767.
[7] J. M. Yang, H. Yang, L. W. Lin, *ACS Nano* **2011**, *5*, 5067 – 5071.
[8] a) L. Shang, S. Dong, G. U. Nienhaus, *Nano Today* **2011**, *6*, 401 – 418; b) Y. Lu, W. Chen, *Chem. Soc. Rev.* **2012**, *41*, 3594 – 3623.
[9] a) C.-C. Huang, C.-T. Chen, Y.-C. Shiang, Z.-H. Lin, H.-T. Chang, *Anal. Chem.* **2009**, *81*, 875 – 882; b) Y. Liu, K. Ai, X. Cheng, L. Huo, L. Lu, *Adv. Funct. Mater.* **2010**, *20*, 951 – 956; c) Y. Wang, Y. Wang, F. Zhou, P. Kim, Y. Xia, *Small* **2012**, *8*, 3769 – 3773.
[10] a) H. M. A. Muhammed, P. Verma, S. Pal, R. Kumar, S. Paul, R. Omkumar, T. Pradeep, *Chem. Eur. J.* **2009**, *15*, 10110 – 10120; b) C. Sun, H. Yang, Y. Yuan, X. Tian, L. Wang, Y. Guo, L. Xu, J. Lei, N. Gao, G. J. Anderson, X.-J. Liang, C. Chen, Y. Zhao, G. Nie, *J. Am. Chem. Soc.* **2011**, *133*, 8617 – 8624; c) L. Shang, N. Azadfar, F. Stockmar, W. Send, V. Trouillet, M. Bruns, D. Gerthsen, G. U. Nienhaus, *Small* **2011**, *7*, 2614 – 2620; d) C. L. Liu, H. T. Wu, Y. H. Hsiao, C. W. Lai, C. W. Shih, Y. K. Peng, K. C. Tang, H. W. Chang, Y. C. Chien, J. K. Hsiao, J. T. Cheng, P. T. Chou, *Angew. Chem.* **2011**, *123*, 7194 – 7198; *Angew. Chem. Int. Ed.* **2011**, *50*, 7056 – 7060.
[11] a) Y. Wang, J. Chen, J. Irudayaraj, *ACS Nano* **2011**, *5*, 9718 – 9725; b) H. Chen, B. Li, X. Ren, S. Li, Y. Ma, S. Cui, Y. Gu, *Biomaterials* **2012**, *33*, 8461 – 8476.
[12] L. Shang, L. Yang, F. Stockmar, R. Popescu, V. Trouillet, M. Bruns, D. Gerthsen, G. U. Nienhaus, *Nanoscale* **2012**, *4*, 4155 – 4160.
[13] M. Baker, *Nat. Methods* **2010**, *7*, 957 – 962.
[14] a) C. Baleizão, S. Nagl, S. M. Borisov, M. Schäferling, O. S. Wolfbeis, M. N. Berberan-Santos, *Chem. Eur. J.* **2007**, *13*, 3643 – 3651; b) D. Cauzzi, R. Pattacini, M. Delferro, F. Dini, C. Di Natale, R. Paolesse, S. Bonacchi, M. Montalti, N. Zaccheroni, M. Calvaresi, F. Zerbetto, L. Prodi, *Angew. Chem.* **2012**, *124*, 9800 – 9803; *Angew. Chem. Int. Ed.* **2012**, *51*, 9662 – 9665.
[15] a) J. M. Forward, D. Bohmann, J. P. Fackler, R. J. Staples, *Inorg. Chem.* **1995**, *34*, 6330 – 6336; b) J. Bomm, C. Günter, J. Stumpe, *J. Phys. Chem. C* **2012**, *116*, 81 – 85; c) Z. Luo, X. Yuan, Y. Yu, Q. Zhang, D. T. Leong, J. Y. Lee, J. Xie, *J. Am. Chem. Soc.* **2012**, *134*, 16662 – 16670.
[16] M. Y. Berezin, S. Achilefu, *Chem. Rev.* **2010**, *110*, 2641 – 2684.
[17] L. Yang, L. Shang, G. U. Nienhaus, *Nanoscale* **2013**, *5*, 1537 – 1543.
[18] L. Treuel, G. U. Nienhaus, *Biophys. Rev.* **2012**, *4*, 137 – 147.
[19] a) C. Röcker, M. Pötzl, F. Zhang, W. J. Parak, G. U. Nienhaus, *Nat. Nanotechnol.* **2009**, *4*, 577 – 580; b) M. P. Monopoli, C. Aberg, A. Salvati, K. A. Dawson, *Nat. Nanotechnol.* **2012**, *7*, 779 – 786; c) L. Shang, S. Brandholt, F. Stockmar, V. Trouillet, M. Bruns, G. U. Nienhaus, *Small* **2012**, *8*, 661 – 665.
[20] a) M. Amelia, R. Flamini, L. Latterini, *Langmuir* **2010**, *26*, 10129 – 10134; b) E. Perevedentseva, N. Melnik, C. Y. Tsai, Y. C. Lin, M. Kazaryan, C. L. Cheng, *J. Appl. Phys.* **2011**, *109*, 034704; c) L. Shang, R. Dörlich, V. Trouillet, M. Bruns, G. U. Nienhaus, *Nano Res.* **2012**, *5*, 531 – 542.
[21] A. E. Nel, L. Madler, D. Velegol, T. Xia, E. M. V. Hoek, P. Somasundaran, F. Klaessig, V. Castranova, M. Thompson, *Nat. Mater.* **2009**, *8*, 543 – 557.
[22] a) M. I. J. Stich, S. Nagl, O. S. Wolfbeis, U. Henne, M. Schaeferling, *Adv. Funct. Mater.* **2008**, *18*, 1399 – 1406; b) J. Feng, K. Tian, D. Hu, S. Wang, S. Li, Y. Zeng, Y. Li, G. Yang, *Angew. Chem.* **2011**, *123*, 8222 – 8226; *Angew. Chem. Int. Ed.* **2011**, *50*, 8072 – 8076; c) J. S. Donner, S. A. Thompson, M. P. Kreuzer, G. Baffou, R. Quidant, *Nano Lett.* **2012**, *12*, 2107 – 2111.
[23] P. N. Hedde, G. U. Nienhaus, *Biophys. Rev.* **2010**, *2*, 147 – 158.

